

Design of HIV-1 Protease Inhibitors Active on Multidrug-Resistant Virus

Dominique L. N. G. Surleraux,[†] Herman A. de Kock,[†] Wim G. Verschuere,[†] Geert M. E. Pille,[†] Louis J. R. Maes,^{†,‡} Anik Peeters,[†] Sandrine Vendeville,[†] Sandra De Meyer,[†] Hilde Azijn,[†] Rudi Pauwels,[†] Marie-Pierre de Bethune,[†] Nancy M. King,[‡] Moses Prabu-Jeyabalan,[‡] Celia A. Schiffer,[‡] and Piet B. T. P. Wigerinck*,[†]

Tibotec BVBA, Generaal de Wittelaan L 11B 3, B-2800 Mechelen, Belgium, and Department of Biochemistry and Molecular Pharmacology, University of Massachusetts Medical School, Worcester, Massachusetts 01605

Received July 9, 2004

On the basis of structural data gathered during our ongoing HIV-1 protease inhibitors program, from which our clinical candidate TMC114 **9** was selected, we have discovered new series of fused heteroaromatic sulfonamides. The further extension into the P2' region was aimed at identifying new classes of compounds with an improved broad spectrum activity and acceptable pharmacokinetic properties. Several of these compounds display an exceptional broad spectrum activity against a panel of highly cross-resistant mutants. Certain members of these series exhibit favorable pharmacokinetic profiles in rat and dog. Crystal structures and molecular modeling were used to rationalize the broad spectrum profile resulting from the extension into the P2' pocket of the HIV-1 protease.

Introduction

Since their introduction in late 1995, HIV-1 protease inhibitors (PIs) have proven to be an advantageous extension of the existing antiretroviral armamentarium, which at the time consisted solely of nucleoside analogue reverse transcriptase inhibitors (NRTIs). This introduction has been marked by a profound decrease in mortality rate associated with HIV-1 infection. Today, PIs are considered as essential components to establish highly active antiretroviral therapy (HAART).^{1,2} HIV-1 protease is a prime target because it is required for HIV-1 replication. Structure-based drug design has led to the discovery of seven approved drugs and several others in advanced clinical trials. Despite this remarkable success, the emergence of HIV-1 mutants that are resistant to current drug regimens remains a critical factor in the clinical failure of antiviral therapy. For the seven currently approved PIs (ritonavir **1**,³ saquinavir **2**,⁴ nelfinavir **3**,⁵ indinavir **4**,⁶ amprenavir **5**,⁷ atazanavir **6**,⁸ and lopinavir **7**⁹) and one PI in development (tipranavir **8**¹⁰) (Figure 1), the emergence of mutants that confer multidrug resistance is disturbing.^{11,12} Increasing cross-resistance has necessitated further research with an emphasis on broad spectrum activity against PI-resistant mutants.

During our HIV-1 protease inhibitors program, efforts directed toward extensive profiling against highly resistant viruses have led to the selection of TMC114 **9**¹³ as our clinical candidate (currently in phase IIB). **9** is a next-generation inhibitor, chemically related to **5**, with an extremely low susceptibility to existing resistant mutants.¹⁴ When **9** is structurally compared to **5**, these two compounds only differ by a second tetrahydrofuran

ring, part of what is termed the bis-THF moiety, present in **9**. The structure and interactions of **9** with HIV-1 protease are shown in Figure 2. The bis-THF moiety present in **9** allows for additional interactions with the Asp29 of the protease,¹⁴ having a profound influence on the antiviral activity. This observation prompted us to extend into P2', where the aniline nitrogen of both **9** and **5** interacts with Asp30, trying to design a next-generation of inhibitors that incorporate structural features that allow for comparable extra interactions with backbone and/or with side chains of amino acids less prone to mutate.

Besides a further advanced broad spectrum activity, new PIs should also have an acceptable oral pharmacokinetic profile (PK) in order to lower pill burden, thereby improving adherence and reducing side effects. Within this scope we explored a large number of annulated heterocyclic sulfonamides as P2' moieties, but this paper will focus only on the most promising ones, the benzothiazole (BT) and benzoxazole (BO) sulfonamides. Crystal structures and calorimetric data were obtained of complexes for one compound from each of these classes, allowing for detailed analysis of the interactions in the P2' pocket.

Chemistry

The first two benzothiazole compounds **10** and **11** were prepared following a described method,¹⁵ using a *p*-aminophenyl precursor to build the fused heterocyclic system via a multistep approach. For the preparation of the benzothiazoles **20a–i** a synthetic route was sought that would give the possibility of modifying the substitution pattern at the C₂–N position of the fused benzothiazoles in a rapid manner. In the first approach a 2-aminobenzothiazole derivative was converted to the 2-chloro analogue using a laborious diazotation step.^{16a} A major improvement could be made when utilizing the good leaving group capacity of the sulfoxide functionality in compounds **18** and **21** (Scheme 1). Starting from

* To whom correspondence should be addressed. Phone: +32 (0)15292445. Fax: +32(0)15401257. Email: pwigeri1@tibbe.jnj.com.

[†] Tibotec BVBA.

[‡] Current address: Faculty of Pharmaceutical, Biomedical and Veterinary Sciences, University of Antwerp, Campus Middelheim, Groenenborgerlaan 171, B-2020 Antwerp, Belgium.

[§] University of Massachusetts Medical School.

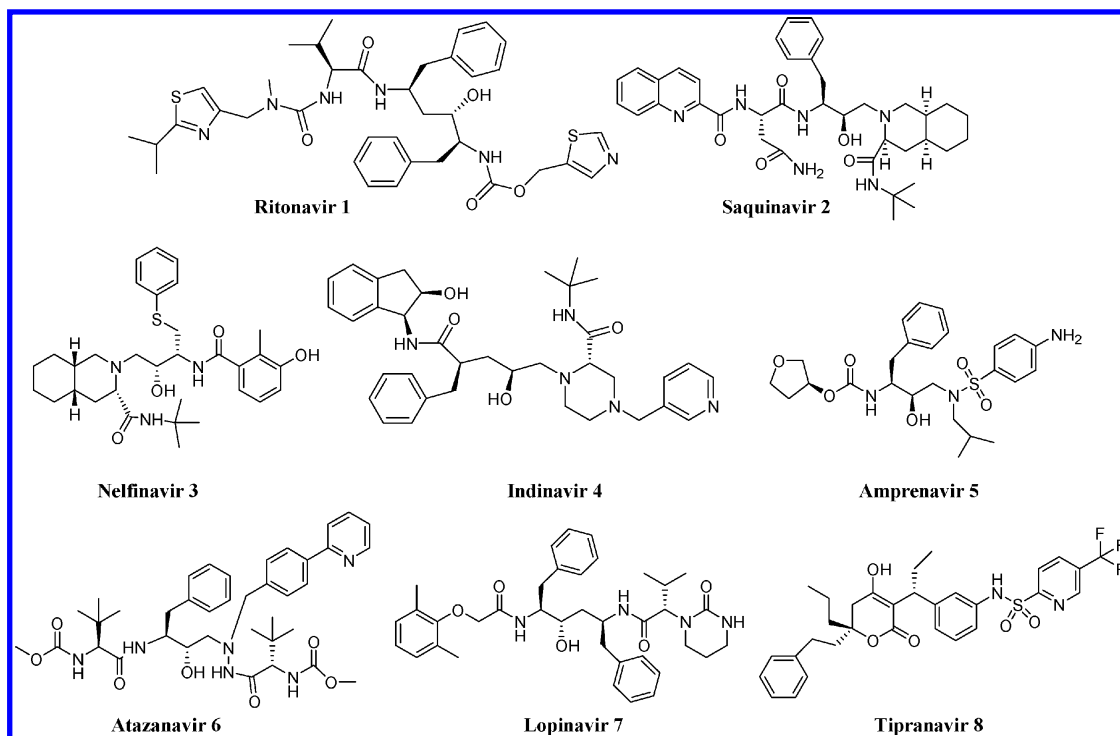


Figure 1. Chemical structure of currently approved HIV-1 protease inhibitors (1–7) and tipranavir (8).

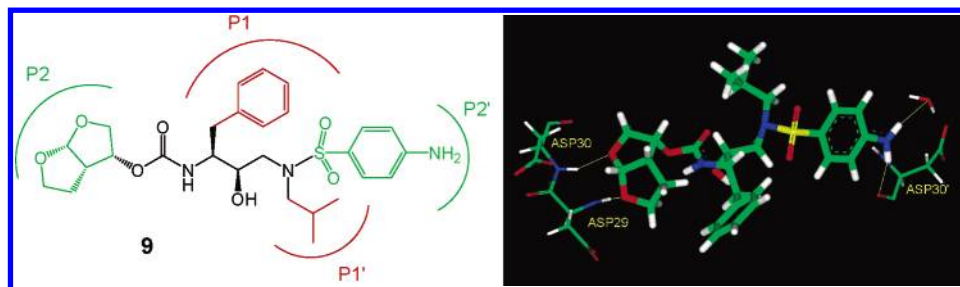


Figure 2. Structure and binding mode of TMC 114 9. Hydrogen bond interactions are shown in P2 and P2' pockets.

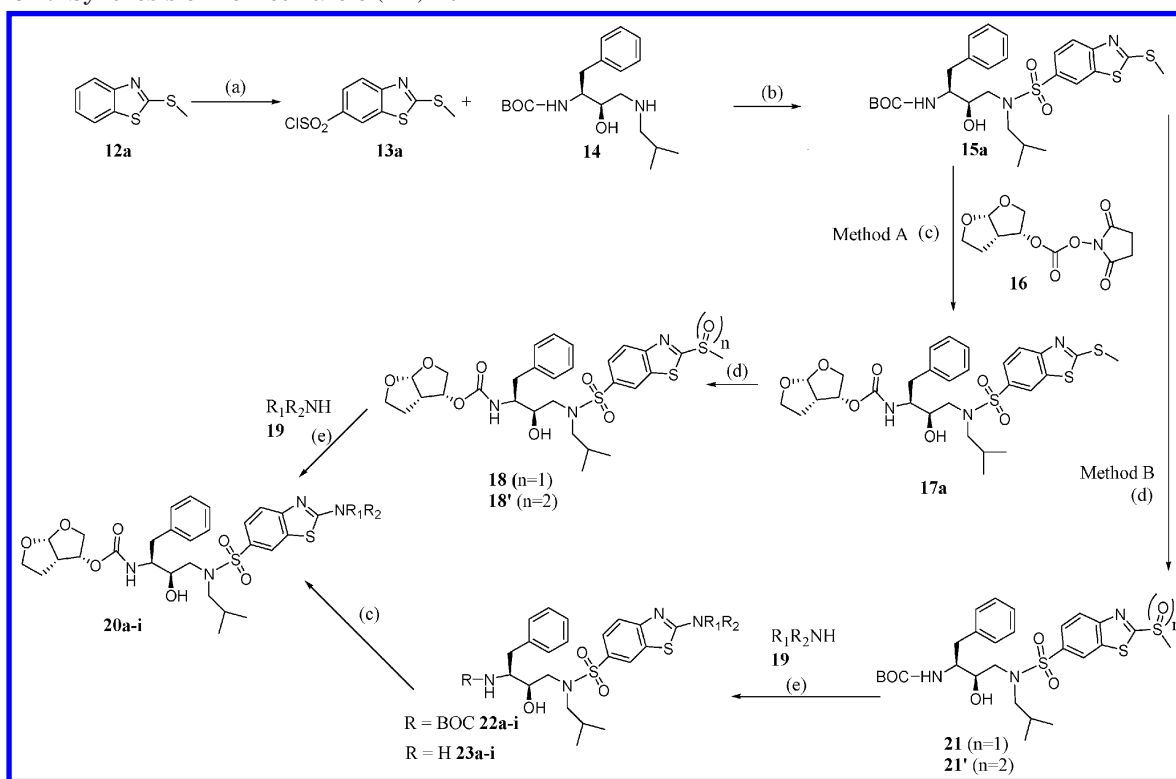
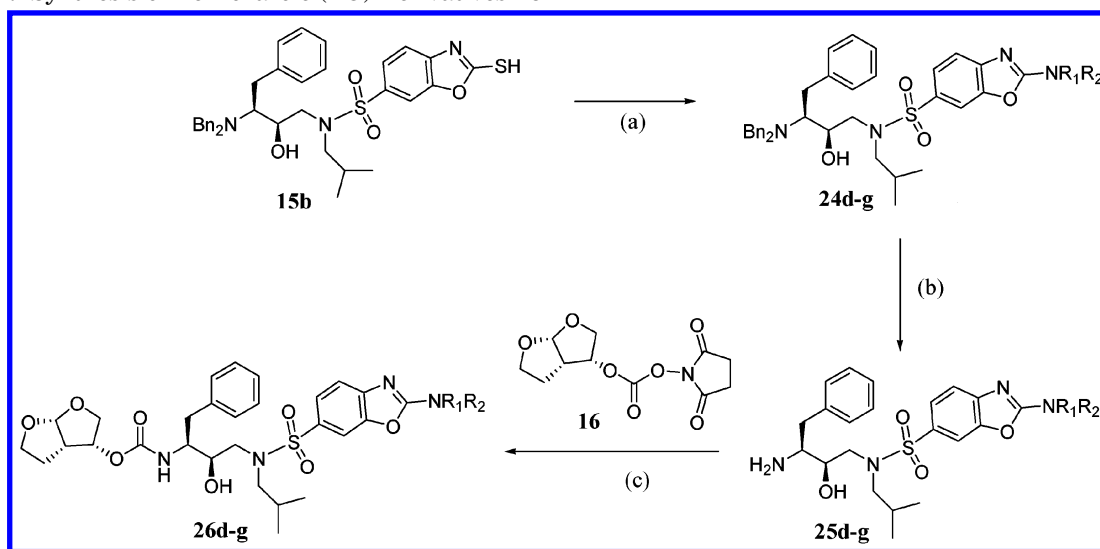
commercially available 2-SMe-benzothiazole **12a** chlorosulfonylation with SOCl_2 and ClSO_3H yielded the desired sulfonyl chloride **13a**. Coupling of **13a** with the known amine **14**¹⁷ gave the intermediate **15a**. Oxidation of the thiomethyl moiety with either MCPBA or magnesium monoperoxophthalate of **15a** (method B) and **17a** (method A) yielded **18/18'** or **21/21'**, respectively, as mixtures of sulfoxide (**18**, **21**) and sulfone (**18'**, **21'**). Intermediate **18** allowed for a one-step synthesis of final compounds (method A). Alternatively, final compounds **20a–i** could be prepared via a two-step procedure (method B).

Benzoxazole compounds **26a–c** were prepared as described earlier.¹⁸ To further evaluate the benzoxazole family, a method similar to the one used for benzothiazole synthesis was developed (Scheme 2). The key intermediate **15b** that allowed relatively fast synthesis was reported earlier by us.¹⁸ Substitution with appropriate amines could be accomplished at elevated temperature (e.g., refluxing acetonitrile). Subsequent debenzoylation of intermediates **24d–g** with Pd/C and H_2 gas followed by coupling of the intermediate amines **25d–g** with **16**¹⁹ gave final compounds **26d–g** in good yield. Further synthetic improvement more resembling the benzothiazole chemistry (Scheme 1) will be published later.

Results and Discussion

In Vitro SAR. All compounds were tested for their antiviral activity against a selected panel of recombinant clinical isolates,²⁰ shown in Table 1. These isolates were selected because of their high degree of cross-resistance to the approved and experimental PIs (Table 2) and because of the presence of mutations in the protease gene associated with resistance to current protease inhibitors as defined by IAS.^{12,21,22} Different combinations of resistance-associated PI mutations were found in each of the selected isolates. Comparing the results for compounds 1–8 (Table 2) with those of our first two benzothiazole compounds **10** and **11** (Table 3) clearly shows a more pronounced antiviral potency for the latter ones, both on wild type as against the selected mutant strains. Although the presence of the exocyclic amino group in **11** seems to lower the activity against wild-type virus compared to **10**, it clearly has a profound influence on retaining the broad spectrum activity across our panel. However, in vivo evaluation of **11** showed poor oral bioavailability, which may in part be correlated with its low aqueous solubility. Another drawback associated with this compound is the high degree of protein binding.²³

Encouraged by the exceptional broad spectrum activity of **11**, we decided to further explore this class of

Scheme 1. Synthesis of Benzothiazole (BT) **20**^a**Scheme 2.** Synthesis of Benzoxazole (BO) Derivatives **26**^a**Table 1.** Resistant Mutant Sequences: Mutations in the Protease Gene Associated with Resistance to PIs According to IAS²¹ in Bold

strain	03	10	11	13	16	19	22	24	32	33	35	36	37	41	43	46	47	50	53	54	55	57	58	62	63	70	71	72	73	77	82	84	85	89	90	93
r13025	I	I							T	M	D		Y			I						R/K	E		P	T	V	V				V		V		
r13034	I	I	I				A/V	I			D	I	T	R/K						V				V	P	V	V				V					
r13363	I								I	F	D	I	N		T	I	V	V			R	K		V	P	L					I		V	M	L	
GSS004421	I	I		V	G/A	I				F			N		I	I	V	V	L	V	R			V	P	V	V	C	V/I	A				M		

2-amino-fused heteroaromatic sulfonamides trying to retain broad spectrum activity while addressing oral bioavailability and protein binding issues.

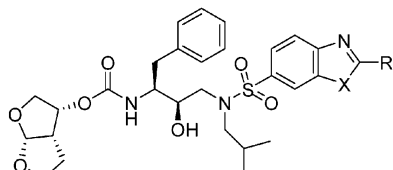
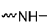

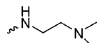
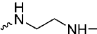
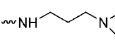
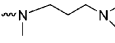
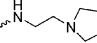
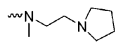
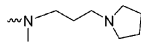


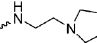
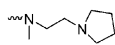
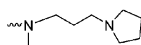
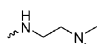
Antiviral results for **20a–i** (BT) and **26a–g** (BO) are presented in Table 3. From these data a few straightforward SAR principles can be put forward:

(i) Replacing the 2- NH_2 function present in **11** and **26a** by either a 2-MeNH (**20a** or **26b**) or a 2-Me₂N (**20b** or **26c**) seems to have a common positive effect on wild-type potency. However, with regard to a maintained broad spectrum activity, the presence of a tertiary substituted C₂-amine in compounds **20b** and **26c** is not

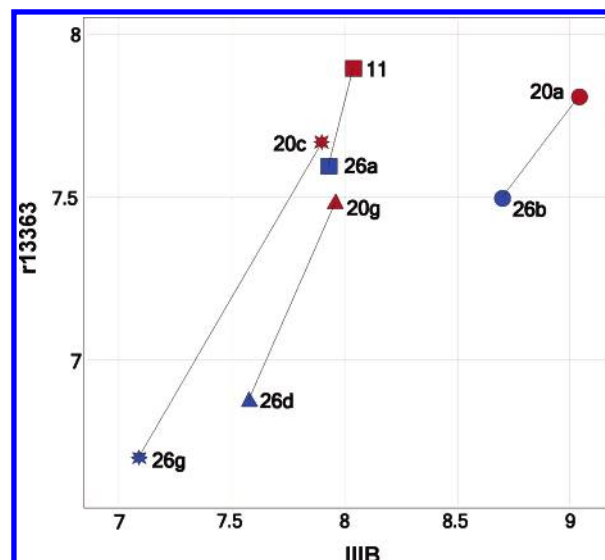
Table 2. Protease Inhibitory Activity (pEC₅₀) and Toxicity (TOX, pCC₅₀) of Currently Approved HIV-1 Protease Inhibitors (1–7) and Tipranavir (8) on Wild Type (IIIB) and Mutant Viruses

	TOX pCC ₅₀	pEC ₅₀				
		IIIB	r13025	r13034	r13363	GSS004421
ritonavir 1	4.53	7.19	5.99	5.30	4.89	4.97
saquinavir 2	4.68	7.58	6.83	5.91	7.54	6.30
nelfinavir 3	4.75	7.15	5.31	5.90	5.82	6.28
indinavir 4	<4.49	7.40	5.97	5.90	6.39	6.47
amprenavir 5	<4.49	7.36	6.43	6.01	4.95	5.75
atazanavir 6	4.53	7.82	5.78	ND	7.23	7.32
lopinavir 7	4.95	8.01	7.84	6.59	6.28	6.02
tipranavir 8	<4.49	6.30	5.74	ND	6.15	6.73

Table 3. Protease Inhibitory Activity (pEC₅₀) and Toxicity (TOX, pCC₅₀) of Compounds of Benzoxazole and Benzothiazole Series on Wild Type (IIIB) and Mutant Viruses

								
	X	R	TOX	IIIB	r13025	r13034	r13363	GSS004421
10	S	H	<4.49	8.96	7.83	8.11	6.57	7.78
11	S	NH ₂	4.77	8.04	8.51	8.42	7.90	8.59
20a	S		<4.49	9.04	8.81	8.81	7.81	8.59
20b	S		<4.49	8.46	7.31	ND	5.36	6.59
20c	S		<4.49	7.95	7.84	8.09	7.67	7.90
20d	S		<4.49	6.68	6.49	6.43	6.11	6.50
20e	S		4.73	7.24	7.69	8.17	7.53	7.72
20f	S		4.68	7.83	6.95	7.32	6.08	6.71
20g	S		<4.49	7.96	7.88	7.91	7.49	7.86
20h	S		4.52	8.25	6.50	6.85	5.64	6.29
20i	S		4.58	7.62	6.16	7.36	5.52	6.81
26a	O	NH ₂	<4.49	7.93	8.21	8.19	7.60	8.06
26b	O		<4.49	8.70	8.13	8.61	7.50	8.07
26c	O		<4.49	8.38	6.66	6.92	5.38	6.58
26d	O		<4.49	7.58	7.12	7.48	6.88	7.21
26e	O		<4.49	7.48	6.65	6.73	5.85	6.55
26f	O		<4.49	7.16	6.63	6.34	5.22	6.22
26g	O		<4.49	7.09	6.87	7.61	6.70	6.81

well tolerated. An analogous trend can be observed for the alkylamino-substituted series when comparing the antiviral activity on mutant strains of compounds **20e**, **20g**, and **26d** with **20f**, **20h**, and **26e**, respectively. The preference of the secondary amines can be explained by the presence of a strong hydrogen bond interaction with the side chain of Asp30' shown in the crystal structures of **20g** and **26b** (see also next paragraph).

**Figure 3.** Scatter plot comparing BO–BT activity on wild type and r13363. BT compounds are shown in red, while BO compounds are shown in blue. Different side chains are presented as different shapes. BT and BO compounds with the same side chain are connected.

(ii) A qualitative analysis of the relationship between the chain length and the antiviral potency showed the ethyl spacer (compounds **20c**, **20h**, and **26e**) to be comparable to the propyl spacer (compounds **20e**, **20i**, and **26f**). The most significant difference is noted on wild-type activity, thus slightly favoring the ethyl spacer.

(iii) Introduction of an alkylamino functionality containing a secondary amine as in compound **20d** has a deleterious impact on antiviral activity, most likely governed by bad cell penetration rather than conflicting interactions with the HIV-1 protease.

(iv) A direct comparison between the benzothiazole and benzoxazole analogues is presented in Figure 3. This graphical representation shows a nearly constant difference in potency between BO and BT analogues, both on wild type and on mutant strain r13363 (strain that shows the most pronounced phenotypic impact across both BO and BT). Making an exception to this generalization are the unbranched compounds **11** and **26a**, showing less variation in activity on both strains. Another observation is that the introduction of alkylamino moieties in the BO class (comparing **26a** with **26g** and **26d**) has a bigger impact on antiviral activity when compared to differences observed for the BT class (comparing **11** with **20c** and **20g**).

Because both the benzoxazole and the benzothiazole series, despite the differences mentioned above, show promising broad spectrum antiviral activity, a subset of compounds was selected and their main properties that could contribute to an improved oral bioavailability were evaluated (in silico/in vitro). The in vitro assays used are well-known and deal with all phases of the ADME process. We have measured the solubility at different pH, the permeability in Caco-2 assay, and the metabolic stability in the presence of rat, dog, and human liver microsomes. Results are presented in Table 4.

Although the cLogP values are well within an acceptable range (2.7–3.9), the calculated polar surface area

Table 4. Results of in Vitro Assays in Comparison with Calculated Properties^a

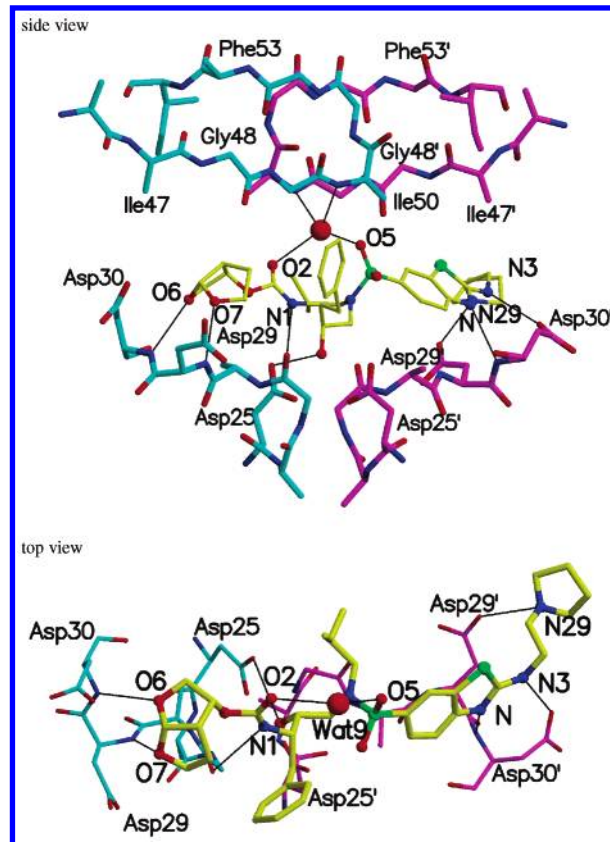
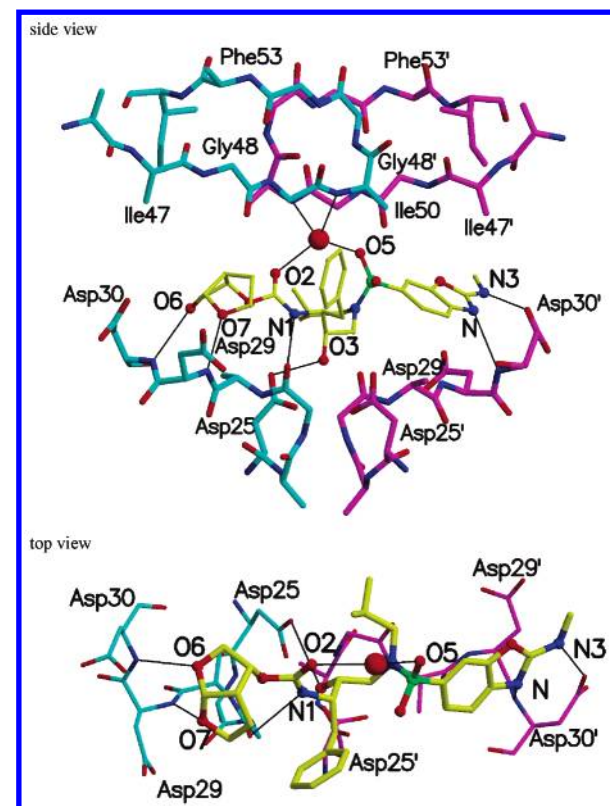
compd	in silico		solubility		metabolic stability			Caco-2	
	CLogP	PSA	pH 7	pH 5	RLM	HLM	DLM	P_{app} Ap-BI	P_{app} Bl-Ap
11	3.26	189.9	<0.01	<0.01	77	65	74	9.9	27.3
20a	3.34	175.9	<0.01	<0.01	72	63	80	19.3	14.2
20c	3.47	179.2	0.04	0.41	19	35	30	6.1	26.6
20f	3.74	170.4	1.18	1.64	47	35	52	2.0	8.5
20g	3.94	179.2	<0.01	0.09	56	26	46	3.5	21.7
26a	2.70	174.8	ND	ND	90	62	67	3.8	23.8
26b	2.78	160.8	<0.01	0.01	70	37	69	17.6	24.0

^a The log *P* and polar surface area (PSA) have been calculated using Scitegic's Pipeline Pilot software. Solubility is determined at pH 7 and pH 5 and expressed in mg/mL. Metabolic stability has been measured in three different species as the percent remaining parent compound after 30 min of incubation with liver microsomes of rat (RLM), dog (DLM), and human (HLM) origin. Apparent permeability in Caco-2 assay is presented in cm/s ($\times 10^6$).

(PSA) values exceed those that are generally accepted (which is around 80 for commercially available orally administered compounds). Starting from compound **11** or **26a**, the introduction of either alkyl (compound **20a** or **26b**) or alkylamino (e.g., compound **20g**) compounds slightly lowers PSA values; however, the introduction of a basic nitrogen (alkylamino series) was mainly directed toward improving aqueous solubility. Comparing the solubility of compounds **20g**, **20f**, and **20c** with that of **11** shows an increased aqueous solubility that is influenced by the substitution pattern around the basic nitrogen. This is illustrated by the solubility at pH 7, which ranges from <0.01 to 1.18 mg/mL going from [2-(1-pyrrolidiny)ethyl]amino in **20g** to [2-(dimethylamino)ethyl]amino in **20c** to [3-(dimethylamino)propyl]methylamino in **20f**. These findings have been further substantiated by more recent findings for both the BT and BO series (data not shown). Metabolic stability in the presence of liver microsomes seems to decrease when introducing the alkylamino moieties, metabolic degradation being the most extensive for human liver microsomes. From the Caco-2 data it is apparent that introduction (starting from compound **11** or **26a**) of a methyl group (compounds **20a** and **26b**) markedly increases the permeability, increasing P_{app} (apical to basolateral) from 9.9 to 19.3 for **20a** and from 3.8 to 17.6 for **26b**. However, the introduction of an alkylamino side chain substantially lowers the apparent permeability (e.g., 3.5 for compound **20g**) besides inducing more pronounced efflux properties.

Crystal Structures of HIV-1 Protease Complexes. For one benzothiazole (**20g**) and one benzoxazole (**26b**) compound presented here, the crystal structure in complex with wild-type HIV-1 protease has been determined to a resolution of 1.83 and 2.00 Å, respectively. The most important hydrogen bond interactions are shown in Figures 4 (**20g**) and 5 (**26b**). The refinement statistics are presented in Table 5. The high resolution of the structures allows for a detailed analysis of the intermolecular interactions present in these complexes.

Hydrogen bonds were calculated for both complexes (Table 6) after the addition of hydrogen atoms. The central water molecule present in the flap region makes hydrogen bonds similar to what has been observed for other HIV-1 protease inhibitors. With the bis-THF moiety present in the P2 pocket, two strong hydrogen

**Figure 4.** Side view and top view of hydrogen bond interactions between **20g** and the enzyme in the P2' pocket.**Figure 5.** Side view and top view of hydrogen bond interactions between **26b** and the enzyme in the P2' pocket.

bonds can be accepted from the backbone of Asp29 and Asp30. The importance of this group has already been reported before. In a recent paper²⁴ the crystal structure of **5** (mono-THF) has been compared to that of **9** (bis-

Table 5. Crystallographic Data Collection and Refinement Statistics for the Complexes of HIV-1 Protease with Compounds **20g** and **26b**

	20g	26b
data collection		
resolution (Å)	1.83	2
<i>a</i> (Å)	50.6	50.7
<i>b</i> (Å)	57.8	58
<i>c</i> (Å)	61.5	62
space group	<i>P</i> 2 ₁ 2 ₁ 2 ₁	<i>P</i> 2 ₁ 2 ₁ 2 ₁
<i>Z</i>	4	4
<i>R</i> _{merge} (%)	5.3	7
completeness (%)	98.7	93.5
temp (K)	210	210
unique reflections	16 311	12 027
total reflections	69 567	30 716
<i>I</i> (σ)	10.5	10.1
refinement		
<i>R</i> factor (%)	18.1	18.2
<i>R</i> free (%)	22.8	23.8
multiple conformations	Q18, E21, D30, D35, I50, G51, Q61, P81, E21', D30', I50', G51', V75'	Q18, E35, K7', E34'
accuracy		
bond length rmsd (Å)	0.03	0.022
bond angle rmsd (deg)	1.423	1.347

Table 6. Hydrogen Bond Distances (in Å) with HIV-1 Protease for **20g** and **26b**^a

	20g	26b
O7...H-N (Asp29)	2.1	2.1
O6...H-N (Asp30)	2.2	2.7
C=O2...H-O-H (flap H ₂ O)	2.1	1.8
S=O5...H-O-H (flap H ₂ O)	1.5	2.0
O3-H...OOC (Asp25)	1.7	2.1
(flap H ₂ O) O...H-N (Ile50)	1.9	2.0
(flap H ₂ O) O...H-N (Ile50')	2.1	2.2
N1-H...O=C (Gly27)	2.5	3.1
N(thia/oxazole)...H-N (Asp30')	2.0	2.6
N3-H...OOC (Asp30')	1.9	2.3
N29(pyrrolidine)...OOC (Asp29')	2.9	

^a Atom numbering for **20g** and **26b** as in Figures 4 and 5, respectively.

THF). For **9**, hydrogen bond distances of 2.0 Å (Asp29) and 2.1 Å (Asp30) were observed. For compound **26b**, the interaction with Asp30 is significantly weaker. For this compound also, the N1-H does not interact with the backbone of Gly27. This is caused by a change in the position of the Gly27 carbonyl group due to an intramolecular hydrogen bond (1.9 Å) formed between the adjacent N-H of Ala28 with one of the catalytic aspartate residues (Asp25). This intramolecular interaction is less pronounced in other crystal structures of HIV-1 protease.

The hydrogen bonds formed with Asp29' and Asp30' are very important because this research effort is focused on optimizing interactions in the P2' pocket. The N atom of the thiazole ring in **20g** interacts with the backbone N-H of Asp30'. The oxazole ring of **26b** is in a similar position as the thiazole ring in **20g**, but the interaction with the backbone of Asp30' is less favorable. Perhaps the presence of a larger sulfur atom in **20g** forces this compound to be located a little lower in the pocket, enhancing the interaction of the N atom with Asp30'. The secondary amine present in both structures forms a strong hydrogen bond interaction with the side chain of Asp30'. This interaction is stronger for **20g** than for **26b** (Table 6, 1.9 and 2.3 Å, respectively). Asp30 is fairly conserved, only mutating to Asn in the presence

Table 7. Thermodynamics of Inhibitor Binding^a

	<i>K</i> _d	Δ <i>H</i>	- <i>T</i> Δ <i>S</i>	Δ <i>G</i>	HB	NROT
5 ^b	3.9 × 10 ⁻¹⁰	-7.3	-5.3	-12.6	8	12
9 ^b	4.5 × 10 ⁻¹²	-12.1	-3.1	-15.2	10	12
TMC126 ^c	3.9 × 10 ⁻¹²	-12	-3.6	-15.6	8	13
20g	6.37 × 10 ⁻¹¹	-11.7	-1.97	-13.67	11	16
26b	9.29 × 10 ⁻¹⁰	-7.3	-4.84	-12.11	7	13

^a Dissociation constant *K*_d is expressed in M; Δ*H*, -*T*Δ*S*, and Δ*G* are given in kcal/mol. The number of hydrogen bond interactions with a donor-acceptor distance of <3.5 Å (HB) and the number of rotatable bonds (NROT) are also shown. ^b Reference 24. ^c Reference 36.

Table 8. In Vivo Assays^a

compd	species	<i>C</i> _{max} (ng/mL)	<i>T</i> _{max} (h)	<i>t</i> _{1/2} (h)	AUC (ng·h/mL)
20f	dog	1680	1.0	2.9	6592
20g	dog	1972	0.5	1.66	6048
26b	dog	986	2.0	0.9	2034
26a	rat	260	1.0	1.6	448
26b	rat	927	1.4	ND	1196

^a Pharmacokinetics in Wistar rats was determined in a single dose study at dose levels of 20 mg/kg. Both compounds were formulated in PEG400. The studies in dog were carried out in coadministration with ritonavir. Data of oral administration to dog were obtained at 20 mg/kg as solution in either PEG400 (**20f** and **26b**) or CD40 + CA (**20g**) (40% w/v hydroxypropyl-β-cyclodextrin with 2% citric acid).

of **3** (in vitro and in vivo). However, an asparagine should still be able to form the same hydrogen bonds to these compounds. Therefore, in terms of the impact of resistance mutations, this interaction can be considered equivalent to a backbone interaction.

For compound **20g** an additional interaction between pyrrolidine and the side chain of Asp29' has been observed. The distance between the pyrrolidine N atom and the closest O atom of the carboxylic acid side chain of Asp29' is 2.9 Å. The pyrrolidine N is likely to be protonated because its estimated p*K*_a is 8.8. Therefore, **20g** and Asp29' likely form a strong hydrogen bond.

Thermodynamics of Inhibitor Binding. In addition, thermodynamic data were collected with isothermal titration calorimetry for the binding of **20g** and **26b** (Table 7). Correlating the thermodynamics of inhibitor binding with crystal structures is very difficult because the binding free energy is an equilibrium between the bound and free forms of both the protease and the inhibitor as well as their changing interactions with the solvent. Nevertheless, we will note a few patterns that we observed between these similar types of inhibitors. The binding free enthalpy (Δ*H*) of **20g** and **26b** is -11.7 and -7.3 kcal/mol, respectively. The higher binding enthalpy measured for **20g** is close to the one reported for **9**²⁴ (-12.1 kcal/mol), which is in agreement with it forming more hydrogen bonds in the crystal structures. This may be explained by the fact that **9** is also capable of making a water-mediated hydrogen bond interaction with the side chain of Asp30' in the P2' pocket.²⁴ In addition, inhibitor **20g**, which contains more degrees of freedom and more rotatable bonds, appears to have the least favorable interaction entropy (Table 7).

In Vivo Results. A limited in vivo evaluation in rat and dog is summarized in Table 8. The pharmacokinetics of **26a** and **26b** in Wistar rats was determined in a single dose study at dose levels of 20 mg/kg. Both compounds were formulated in PEG400. After oral administration, **26b** showed a higher *C*_{max} than **26a** by

3.5-fold. These results correlate nicely with the observed difference between the apparent permeability of **26a** ($P_{app} = 3.8$) and **26b** ($P_{app} = 17.6$). The studies in dog were carried out in coadministration with ritonavir because the systemic availability can be "boosted" considerably through inhibition of P450 metabolism (e.g., first-pass effect and metabolic clearance), a principle used with lopinavir in the commercial preparation Kaletra. While compound **11** showed low systemic availability after oral dosing, we hoped to improve on oral bioavailability with limited impact on the antiviral spectrum. Data of oral administration to dog at 20 mg/kg as a solution in either PEG400 (**20f** and **26b**) or CD40 + CA (**20g**) (40% w/v hydroxypropyl- β -cyclodextrin with 2% citric acid) are presented in Table 8. The results clearly indicate that for both BO and BT families, acceptable oral PK can be attained. Peak plasma levels as high as 1972 and 1680 ng/mL were observed for **20g** and **20f**, respectively. These data warranted a further exploration of both families. Moreover, as mentioned before, the substitution pattern around the basic nitrogen has a significant influence on the aqueous solubility and hence also influences the systemic availability. Recent findings show that further improvement seems possible. These will be published in due course.

Conclusion

In summary, using structural information obtained during our continuing HIV-1 protease program, we have designed and synthesized novel series of fused heterocyclic sulfonamides. The pronounced broad spectrum activity of one of our first compounds in the benzothiazole series **11** encouraged us to further explore fused heterocyclic sulfonamide inhibitors that extend further into the P2' region of the HIV-1 protease. Synthetic improvements that allow for fast preparation of a diverse set of compounds were developed for both the benzothiazole and benzoxazole series. In vitro results demonstrate that incorporation of a heterocyclic part in P2' can result in a substantial increase in the broad spectrum against highly PI-resistant mutants. Against r13363, containing no less than seven resistance-associated protease mutations, several of our compounds maintain an activity in the range of 7.5–8 (pEC_{50}). Crystal structures and molecular modeling were used to rationalize the broad spectrum profile resulting from the extension into the P2' pocket of the HIV-1 protease.

In vitro and in vivo evaluation of ADME properties was done in parallel with our synthesis program and delivered a set of compounds with better physical properties (i.e., solubility, protein binding). Peak plasma levels as high as 1972 and 1680 ng/mL were observed for **20g** and **20f**, respectively. Despite the need for boosting, these compounds proved to be well absorbed in animal species and could be candidates for further development.

Experimental Section

Chemistry. General Experimental Procedures. NMR spectra were recorded on a Bruker Avance 400 spectrometer, operating at 400 MHz for 1H and 100 MHz for ^{13}C and with DMSO as solvent unless otherwise stated. In every case tetramethylsilane (TMS) was used as an internal standard. Chemical shifts are given in ppm, and J values are given in Hz. Multiplicity is indicated using the following abbrevia-

tions: d for doublet, t for a triplet, m for a multiplet, etc. For the sake of brevity, it was opted to completely characterize (NMR included) one representative example of each subset of compounds. Low-resolution mass spectra (LRMS) were obtained from a single quadrupole (Waters ZMD), ion trap (ThermoFinnigan LCQ Deca), or time-of-flight (Waters LCT) mass spectrometer using electrospray ionization (ESI) in positive or negative mode. All reagents were purchased from commercial sources (Acros, Aldrich, etc.) and were used as received. Column chromatography was carried out on silica gel 60 Å, 60–200 μm (ROCC). Thin-layer chromatography was performed on silica gel 60 F₂₅₄ plates (Merck). Optical rotations were measured at the sodium D line, using a Propol automatic polarimeter. Analytical HPLC was done on a Waters Alliance 2690 (pump + autosampler) system equipped with a Waters 996 photodiode array detector. To check the purity of the end products (**20** and **26**), two independent chromatographic systems were used.

The first system consisted of the following: column, Waters Xterra MS C18, (3.5 μm , 4.60 mm \times 100 mm); mobile phase A, 10 mM CH_3COONH_4 in H_2O ; mobile phase B, CH_3CN . Analyses were run at 30 $^\circ C$ using a flow rate of 1 mL/min and applying the following gradient: 0 min, 5% mobile phase B; 10 min, 95% mobile phase B; 12 min, 95% mobile phase B. In every case, 10 μL of a 1 mM solution was injected. The equilibration time between two runs was 3 min.

The second system (polar) consisted of the following: column, Alltech Prevail C18 (3.0 μm , 4.6 mm \times 100 mm); mobile phase A, 10 mM CH_3COONH_4 in H_2O ; mobile phase B, CH_3CN . Analyses were run at 30 $^\circ C$ using a flow rate of 1 mL/min and applying the following gradient: 0 min, 0% mobile phase B; 1 min, 0% mobile phase B; 9 min, 95% mobile phase B; 12 min, 95% mobile phase B. In every case, 10 μL of a 1 mM solution was injected. The equilibration time between two runs was 3 min.

Eluted peaks were detected at a single wavelength (λ_{max}) for both chromatographic systems. The retention time for each compound is given for both systems and is reported in minutes. A full table with retention time and purity (%) is in Supporting Information.

Synthesis of Compound 20g. To a 0.5 M solution of sulfoxide **18** (22.5 mmol) in DCM was added 3 equiv of aminoethylpyrrolidine. This solution was refluxed for 1.5 h, washed with a saturated $NaHCO_3$ solution, dried over $MgSO_4$, and filtered over dicalite. Evaporation of solvent and purification on silica provided compound **20g** (12.02 g, 76%). MS (m/z): 702 (MH^+). 1H NMR and ^{13}C NMR spectra of **20g** can be found in Supporting Information.

Synthesis of Compound 26d. To a solution of amine **25d** (10 mmol) in DCM (20 mL) at 0 $^\circ C$ was added 13 mmol of triethylamine and 12 mmol of 2,5-pyrrolidinedione-1-[[3*R*,-3*aS*,6*aR*]-hexahydrofuro[2,3-*b*]furan-3-yl]oxy] **16**. The reaction mixture was then stirred at room temperature for 3 h, then washed with a saturated $NaHCO_3$ solution. The organic phase was dried over $MgSO_4$ and evaporated. Residue was then purified by column chromatography. Upon concentrating the suitable fractions, compound **26d** was isolated (3.56 g, 52%). MS (m/z): 686 (MH^+). The 1H NMR spectrum of **26d** can be found in Supporting Information.

Virology. Cell-Based Anti-HIV and Toxicity Assay. The antiviral activity has been determined with a cell-based replication assay. This assay directly measures the ongoing replication of virus in MT4 cells via the specific interaction of HIV-tat with LTR sequences coupled to GFP. In the toxicity assay, a reduced expression of the GFP reporter protein serves as a marker for cellular toxicity of a compound. Briefly, various concentrations of the test compounds are brought into a 384-well microtiter plate. Subsequently, MT4 cells and HIV-1/LAI (wild type) are added to the plate at a concentration of 150 000 cells/mL and 200 cell culture infectious doses 50% (CCID₅₀). To determine the toxicity of the test compound, mock-infected cell cultures containing an identical compound concentration range are incubated for 3 days (37 $^\circ C$, 5% CO_2) in parallel with the HIV-infected cell cultures. On the basis of the calculated

percent inhibition for each compound concentration, dose response curves are plotted and EC₅₀, pEC₅₀, CC₅₀, and pCC₅₀ values are calculated.

Activity in the Presence of Human Serum and Human Serum Proteins. MT4-LTR-EGFP cells were infected with HIV-1/LAI at a MOI of 0.001–0.01 CCID₅₀ per cell. After 1 h of incubation, cells were washed and plated into a 384-well plate containing serial dilutions of the compound in the presence of 10% FCS or 10% FCS + 50% human serum (HS). After 3 days of incubation, the relative fluorescence of treated cultures was measured and compared with the relative fluorescence of untreated cultures. The EC₅₀ of a compound was defined as the concentration that inhibited the relative fluorescence by 50%.

Metabolic Stability. The metabolic stability was determined in dog, human, and rat liver microsomes (10 μ M compound, 30 and 120 min incubation at 37 °C). The degree of metabolism is determined by direct measurement of the residual parent compound in the reaction mixture using LC-MS (liquid chromatography–mass spectrometry).

Protein Crystallography. Protein expression, isolation, and purification were carried out as previously described.²⁵ The protein used for crystallizing the inhibitors was further purified using a Pharmacia Superdex 75 FPLC column.

Crystall screens were set up by the hanging drop vapor diffusion method as described elsewhere.²⁶ The inhibitors were dissolved in dimethyl sulfoxide (DMSO). A protein concentration of 1 mg/mL was used for crystallization by adding 3 molar excess of the inhibitors. The reservoir and the precipitant solutions contained 126 mM sodium phosphate at pH 6.2, 63 mM sodium citrate, and 27–35% AMSO4. Crystals of longest dimension, 0.2 mm, appeared in 2–3 days.

Intensity data were collected at the in-house (University of Massachusetts Medical School) R-axis IV image plate, mounted on a Rigaku X-ray generator delivering X-rays at a power rating of 50 kV/100 mA. Data collection was carried out at –80 °C. Data processing was carried out using Denzo and ScalePack.^{27,28} Data collection statistics are listed in Table 5.

Structure determination was carried out by AMoRe²⁹ using the CCP4i interface.³⁰ Crystallographic refinement included water picking using ARP/wARP³¹ and positional refinement using Crystallography and NMR System (CNS)³² and Refmac 5.³³ Model building was performed using the interactive graphics program CHAIN.³⁴ The final refinement statistics are provided in Table 5.

Isothermal Titration Calorimetry. Thermodynamic parameters of inhibitor binding were determined using an isothermal titration calorimeter, VP-ITC (MicroCal Inc., Northampton, MA). The buffer used for all protease and inhibitor solutions consisted of 10 mM sodium acetate, pH 5.0, 2% DMSO, and 2 mM tris(2-carboxyethyl)phosphine (TCEP). The binding affinities of **20g** and **26b** were obtained by the displacement titration method, using acetylpepstatin (300 μ M) as the weaker binder.^{35,36} For experiments with **20g**, 32 or 24 injections of 9 μ L each of pepstatin were injected into the calorimetric cell containing 13 or 9 μ M protease, respectively. This was followed by 9 or 7 μ L injections of 125 μ M **20g** to saturation. For experiments with **26b**, 36 injections of 8 μ L each were injected into the cell containing protease in the range of 18–21 μ M, followed by 6 μ L injections of 200 μ M **26b** to saturation. Each experiment was performed at least twice. Heats of dilution were subtracted from the corresponding heats of reaction to obtain the heat due solely to inhibitor binding to the enzyme. Data were processed using the Origin 7 software package from Microcal.

Modeling. The crystal structures have some missing and disordered side chains and do not contain information on the position of the hydrogen atoms. Therefore, the structures were first completed by adding the missing hydrogen atoms and side chains using the Biopolymer module in InsightII (Accelrys Inc). This was followed by an optimization of the hydrogen atoms using the conjugate gradient approach. The CVFF force field³⁷ was used in the Discover module of InsightII to perform these

optimizations. The refinement was finished when the largest derivative was smaller than 0.01.

Acknowledgment. M.P.-J., N.M.K., and C.A.S. were supported by the National Institutes of Health (Grant P01-GM66524) and Tibotec/COSAT. We thank Liesbet J. Smeulders and Inge M. J. Vereycken for performing the antiviral assays, Marleen J. M. Van Dooren for analytical support, and Vincent Chou for assistance with the crystallographic refinement.

Supporting Information Available: Experimental details for the synthetic procedures and characterization data for intermediate and final compounds. This material is available free of charge via the Internet at <http://pubs.acs.org>.

References

- (1) Bartlett, J. A.; DeMasi, R.; Quinn, J.; Moxham, C.; Rousseau, F. Overview of the effectiveness of triple combination therapy in antiretroviral-naïve HIV-1 infected adults. *AIDS* **2001**, *15*, 1369–1377.
- (2) Gulick, R. M.; Mellors, J. W.; Havlir, D.; Eron, J. J.; Meibohm, A.; Condra, J. H.; Valentine, F. T.; McMahon, D.; Gonzalez, C.; Jonas, L.; Emini, E. A.; Chodakewitz, J. A.; Isaacs, R.; Richman, D. D. 3-year suppression of HIV viremia with indinavir, zidovudine, and lamivudine. *Ann. Intern. Med.* **2000**, *133*, 35–39.
- (3) Xiaoli, C.; Lin, L.; Kempf, D. J.; Hing, S.; Wideburg, N. E.; Saldivar, A.; Vasavanonda, S.; Marsh, K. C.; McDonald, E.; Norbeck, D. W. Evaluation of furofuran as a P₂ ligand for symmetry-based HIV protease inhibitors. *Bioorg. Med. Chem. Lett.* **1996**, *6*, 2847–2852.
- (4) Roberts, N. A.; Martin, J. A.; Kington, D.; Broadhurst, A. V.; Craig, J. C.; Duncan, I. B.; Galpin, S. A.; Handa, B. K.; Kay, J.; Krohn, A. Rational design of peptide-based HIV proteinase inhibitors. *Science* **1990**, *248*, 358–361.
- (5) Kaldor, S. W.; Kalish, V. J.; Davies, J. F.; Shetty, B. V.; Fritz, J. E.; Appelt, K.; Burgess, J. A.; Campanale, K. M.; Chirgadze, N. Y.; Clawson, D. K.; Dressman, B. A.; Hatch, S. D.; Khalil, D. A.; Kosa, M. B.; Lubbehusen, P. P.; Muesing, M. A.; Patlick, A. K.; Reich, S. H.; Su, K. S.; Tatlock, J. H. Viracept (Nelfinavir Mesylate, AG1343): A Potent, Orally Bioavailable Inhibitor of HIV-1 Protease. *J. Med. Chem.* **1997**, *40*, 3979–3985.
- (6) Dorsey, B. D.; Levin, R. B.; McDaniel, S. L.; Vacca, J. P.; Guare, J. P.; Darke, P. L.; Zugay, J. A.; Emini, E. A.; Schleif, W. A.; Quintero, J. C.; Lin, J. H.; Chen, L.-W.; Holloway, M. K.; Fitzgerald, P. M. D.; Axel, M. G.; Ostovic, D.; Anderson, P. S.; Huff, J. R. L-735,524: the design of a potent and orally bioavailable HIV protease inhibitor. *J. Med. Chem.* **1994**, *37*, 3443–3451.
- (7) Kim, E. E.; Baker, C. T.; Dwyer, M. D.; Murcko, M. A.; Rao, B. G.; Tung, R. D.; Navia, M. A. Crystal structure of HIV-1 protease in complex with VX-478, a potent and orally bioavailable inhibitor of the enzyme. *J. Am. Chem. Soc.* **1995**, *117*, 1181–1182.
- (8) Robinson, B. S.; Riccardi, K. A.; Gong, Y. F.; Guo, Q.; Stock, D. A.; Blair, W. S.; Terry, B. J.; Deminie, C. A.; Djang, F.; Colonno, R. J.; Lin, P. F. BMS-232632, a highly potent human immunodeficiency virus protease inhibitor that can be used in combination with other available antiretroviral agents. *Antimicrob. Agents Chemother.* **2000**, *44*, 2093–2099.
- (9) Sham, H. L.; Kempf, D. J.; Molla, A.; Marsh, K. C.; Kumar, G. N.; Chen, C. M.; Kati, W.; Stewart, K.; Lal, R.; Hsu, A.; Betebenner, D.; Korniyeva, M.; Vasavanonda, S.; McDonald, E.; Saldivar, A.; Wideburg, N.; Chen, X.; Niu, P.; Park, C.; Jayanti, V.; Grabowski, B.; Granneman, G. R.; Sun, E.; Japour, A. J.; Norbeck, D. W. ABT-378, a highly potent inhibitor of the human immunodeficiency virus protease. *Antimicrob. Agents Chemother.* **1998**, *42*, 3218–3224.
- (10) Turner, S. R.; Strohbach, J. W.; Tommasi, R. A.; Aristoff, P. A.; Johnson, P. D.; Skulnick, H. I.; Dolak, L. A.; Seest, E. P.; Tomich, P. K.; Bohanon, M. J.; Horng, M. M.; Lynn, J. C.; Chong, K. T.; Hinshaw, R. R.; Watenpaugh, K. D.; Janakiraman, M. N.; Thaisrivongs, S. Tipranavir (PNU-140690): a potent, orally bioavailable nonpeptidic HIV protease inhibitor of the 5,6-dihydro-4-hydroxy-2-pyrone sulfonamide class. *J. Med. Chem.* **1998**, *41*, 3467–3476.
- (11) Condra, J. H.; Schleif, W. A.; Blahy, O. M.; Gabryelski, L. J.; Graham, D. J.; Quintero, J. C.; Rhodes, A.; Robbins, H. L.; Roth, E.; Shivaprakash, M. In vivo emergence of HIV-1 variants resistant to multiple protease inhibitors. *Nature* **1995**, *374*, 569–571.
- (12) Clavel, F.; Hance, A. J. HIV drug resistance. Structural and thermodynamic basis of resistance to HIV-1 protease inhibition: Implications for inhibitor design. *N. Engl. J. Med.* **2004**, *350*, 1023–1035.

- (13) Koh, Y.; Nakata, H.; Maeda, K.; Ogata, H.; Bilcer, G.; Devasamudram, T.; Kincaid, J. F.; Boross, P.; Wang, Y.-F.; Tie, Y.; Volarath, P.; Gaddis, L.; Harrison, R. W.; Weber, I. T.; Ghosh, A. K.; Mitsuya, H. Novel bis-tetrahydrofuranylurethane-containing nonpeptidic protease inhibitor (PI) UIC-94017 (TMC114) with potent activity against multi-PI-resistant human immunodeficiency virus in vitro. *Antimicrob. Agents Chemother.* **2003**, *47*, 3123–3129.
- (14) Ghosh, A. K.; Kincaid, J. F.; Walters, D. E.; Chen, Y.; Chaudhuri, N. C.; Thompson, W. J.; Culberson, C.; Fitzgerald, P. M. D.; Lee, H. Y.; McKee, S. P.; Munson, P. M.; Duong, T. T.; Darke, P. L.; Zugay, J. A.; Schleif, W. A.; Axel, M. G.; Lin, J.; Huff, J. R. Nonpeptidic P2 Ligands for HIV Protease Inhibitors: Structure-Based Design, Synthesis, and Biological Evaluation. *J. Med. Chem.* **1996**, *39*, 3278–3290.
- (15) (a) Nagarajan, S. R.; De Crescenzo, G. A.; Getman, D. P.; Lu, H.-F.; Sikorski, J. A.; Walker, J. L.; McDonald, J. J.; Houseman, K. A.; Kocan, G. P.; Kishore, N.; Mehta, P. P.; Funkes-Shippy, C. L.; Blystone, L. Discovery of novel benzothiazolesulfonamides as potent inhibitors of HIV-1 protease. *Bioorg. Med. Chem.* **2003**, *11*, 4769–4777. (b) Kunda, S. A.; Letendre, L. J.; De Crescenzo, G. A. Synthesis of benzo-fused heterocyclic sulfonyl chlorides for preparation of amino acid hydroxyethylamine sulfonamide retroviral protease inhibitors. U.S. Patent 6140505, 2000; CAN 133:322130, 2000.
- (16) (a) Surleraux, D. L. N. G.; Wigerinck, P. T. B. P.; Getman, D. P. Broad-spectrum 2-aminobenzothiazole sulfonamide HIV protease inhibitors. PCT Int. Appl. WO 2004/014371, 2004; CAN 140:193033, 2004. (b) Surleraux, D. L. N. G.; Wigerinck, P. T. B. P.; Getman, D.; Verschuere, W. G.; Vendeville, S.; de Bethune, M.-P.; De Kerpel, J. O. A.; Moors, S. L. C.; de Kock, H. A.; Voets, M. C. J. Broad-spectrum 2-(substituted-amino)-benzothiazole-sulfonamide HIV protease inhibitors. PCT Int. Appl. WO 2002/083657, 2002; CAN 137:325410, 2002. (c) Vazquez, M. L.; Mueller, R. A.; Talley, J. J.; Getman, D. P.; Decrescenzo, G. A.; Freskos, J. N.; Bertenshaw, D. E.; Heintz, R. M. Amino acid hydroxyethylamine sulfonamides useful as retroviral protease inhibitors. U.S. Patent 5968942, 1999; CAN 131:295568, 1999. (d) Sikorski, J. A.; Getman, D. P.; Decrescenzo, G. A.; Devadas, B.; Freskos, J. N.; Lu, H.-F.; McDonald, J. J. Preparation of substituted sulfonylalkanylamino hydroxyethylamine sulfonamide retroviral protease inhibitors. U.S. Patent 5753660, 1998; CAN 129:16390, 1998. (e) Sikorski, J. A.; Getman, D. P.; Decrescenzo, G. A.; Devadas, B.; Freskos, J. N.; Lu, H.-F.; McDonald, J. J. Preparation of *N*-[2-hydroxy-4-phenyl-3-(sulfonylalkanylamino)butyl]arylsulfonamides and analogs as retroviral protease inhibitors. PCT Int. Appl. WO 97/18205, 1997; CAN 127:65754, 1997.
- (17) (a) Kunda, S. A.; Letendre, L. J.; De Crescenzo, G. A. Benzo fused heterocyclic sulfonyl halide intermediates for the preparation of amino acids as HIV protease inhibitors. PCT Int. Appl. WO 99/59989, 1999; CAN 132:6692, 1999. (b) Getman, D. P.; Decrescenzo, G. A.; Freskos, J. N.; Vazquez, M. L.; Sikorski, J. A.; Devadas, B.; Nagarajan, S.; Brown, D. L.; McDonald, J. J. Preparation of *N*-heterocyclecarbonyl amino acid hydroxyethylamine sulfonamide as retroviral protease inhibitors. PCT Int. Appl. WO 96/28465, 1996; CAN 126:31657, 1996. (c) Getman, D. P.; Decrescenzo, G. A.; Freskos, J. N.; Vasquez, M. L.; Sikorski, J. A.; Devadas, B.; Nagarajan, S.; Brown, D. L.; McDonald, J. J. Preparation of bisamino acid hydroxyethylaminosulfonamide retroviral protease inhibitors. PCT Int. Appl. WO 96/28464, 1996; CAN 126:8710, 1996.
- (18) (a) Surleraux, D. L. N. G.; Vendeville, S. M. H.; Verschuere, W. G.; de Bethune, M.-P. T. M. M. G.; de Kock, H. A.; Tahri, A. Preparation of 2-amino-benzoxazole sulfonamide as broad-spectrum HIV protease inhibitors. PCT Int. Appl. WO 2002/092595, 2002; CAN 137:384835, 2002. (b) Surleraux, D. L. N. G.; Vendeville, S. M. H.; Verschuere, W. G.; de Bethune, M.-P. T. M. M. G.; de Kock, H. A.; Tahri, A.; Erra S. M. Preparation of 2-(substituted-amino)benzoxazole sulfonamides as broad spectrum HIV protease inhibitors. PCT Int. Appl. WO 2002/081478, 2002; CAN 137:310904, 2002.
- (19) Takeda, K.; Akagi, Y.; Saiki, A.; Tsukahara, T.; Ogura, H. Studies on activating methods of functional groups. Part X. Convenient methods for syntheses of active carbamates, ureas and nitrosoureas using *N,N'*-disuccinimido carbonate (DSC). *Tetrahedron Lett.* **1983**, *24*, 4569–4572.
- (20) Hertogs, K.; de Bethune, M. P.; Miller, V.; Ivens, T.; Schel, P.; Van Cauwenberge, A.; Van Den Eynde, C.; Van Gerwen, V.; Azijn, H.; Van Houtte, M.; Peeters, F.; Staszewski, S.; Conant, M.; Bloor, S.; Kemp, S.; Larder, B.; Pauwels, R. A rapid method for simultaneous detection of phenotypic resistance to inhibitors of protease and reverse transcriptase in recombinant human immunodeficiency virus type 1 isolates from patients treated with antiretroviral drugs. *Antimicrob. Agents Chemother.* **1998**, *42*, 269–276.
- (21) Johnson, V. A.; Brun-Vézinet, F.; Clotet, B.; Conway, B.; D'Aquila, R. T.; Demeter, L. M.; Kuritzkes, D. R.; Pillay, D.; Schapiro, J. M.; Telenti, A.; Richman, D. D. Update of the Drug Resistance Mutations in HIV-1: 2004. *Top. HIV Med.* **2004**, *12*, 119–124.
- (22) Velazquez-Campoy, A.; Muzammil, S.; Ohtaka, H.; Schoen, A.; Vega, S.; Freire, E. Structural and thermodynamic basis of resistance to HIV-1 protease inhibition: Implications for inhibitor design. *Curr. Drug Targets: Infect Disord.* **2003**, *3*, 311–328.
- (23) (a) Koeplinger, K. A.; Zhao, Z. Chromatographic measurement of drug–protein interaction: determination of HIV protease inhibitor–serum albumin association. *Anal. Biochem.* **1996**, *243*, 66–73. (b) Schon, A.; Ingaramo, M. d. M.; Freire, E. The binding of HIV-1 protease inhibitors to human serum proteins. *Biophys. Chem.* **2003**, *105*, 221–230.
- (24) King, N. M.; Prabu-Jeyabalan, M.; Nalivaika, E. A.; Wigerinck, P.; de Bethune, M.-P.; Schiffer, C. A. The structural and thermodynamic basis for the binding of TMC114, a next-generation HIV-1 protease inhibitor. *J. Virol.* **2004**, *78*, 12012–12021.
- (25) King, N. M.; Melnick, L.; Prabu-Jeyabalan, M.; Nalivaika, E. A.; Yang, S.-S.; Gao, Y.; Nie, X.; Zepp, C.; Heffner, D. L.; Schiffer, C. A. Lack of synergy for inhibitors targeting a multi-drug-resistant HIV-1 protease. *Protein Sci.* **2002**, *11*, 418–429.
- (26) Prabu-Jeyabalan, M.; Nalivaika, E. A.; King, N. M.; Schiffer, C. A. Viability of a drug-resistant HIV-1 protease variant: structural insights for better anti-viral therapy. *J. Virol.* **2003**, *77*, 1306–1315.
- (27) Minor, W. *XDISPLAYF* (program); Purdue University: West Lafayette, IN, 1993.
- (28) Otwinowski, Z.; Minor, W. Processing of X-ray diffraction data collected in oscillation mode. *Macromolecular Crystallography Part A*; Academic Press: New York, 1997; pp 307–326.
- (29) Navaza, J. AmoRe: an automated package for molecular replacement. *Acta Crystallogr.* **1994**, *A50*, 157–163.
- (30) Collaborative-Computational-Project, N. The CCP4 suite: programs for protein crystallography. *Acta Crystallogr.* **1994**, *D50*, 760–763.
- (31) Morris, R. J.; Perrakis, A.; Lamzin, V. S. ARP/wARP's model-building algorithms. I. The main chain. *Acta Crystallogr.* **2002**, *D58*, 968–975.
- (32) Brünger, A. T.; Adams, P. D.; Clore, G. M.; DeLano, W. L.; Gros, P.; Grosse-Kunstleve, R. W.; Jiang, J. S.; Kuszewski, J.; Nilges, M.; Pannu, N. S.; Read, R. J.; Rice, L. M.; Simonson, T.; Warren, G. L. Crystallography & NMR system: A new software suite for macromolecular structure determination. *Acta Crystallogr.* **1998**, *D54*, 905–921.
- (33) Murshudov, G. N.; Vagin, A. A.; Dodson, E. J. Refinement of macromolecular structures by the maximum-likelihood method. *Acta Crystallogr.* **1997**, *D53*, 240–255.
- (34) Sack, J. S. CHAIN—a crystallographic modeling program. *J. Mol. Graphics* **1988**, *6*, 224–225.
- (35) Sigurskjold, B. Exact analysis of competition ligand binding by displacement isothermal titration calorimetry. *Anal. Biochem.* **2000**, *277*, 260–266.
- (36) Velazquez-Campoy, A.; Kiso, Y.; Freire, E. The binding energetics of first- and second-generation HIV-1 protease inhibitors: implications for drug design. *Arch. Biochem. Biophys.* **2001**, *390*, 169–175.
- (37) Dauber-Osguthorpe, P.; Roberts, V. A.; Osguthorpe, D. J.; Wolff, J.; Genest, M.; Hagler, A. T. Structure and energetics of ligand binding to proteins: *E. coli* dihydrofolate reductase-trimethoprim, a drug–receptor system. *Proteins: Struct., Funct., Genet.* **1988**, *4*, 31–47.

JM049454N